

# Nonadiabatic Noncyclic Geometric Quantum Computation via unconventional Rydberg blockade

Bao-Jie Liu,<sup>1,2</sup> Shi-Lei Su,<sup>3,\*</sup> and Man-Hong Yung<sup>2,†</sup>

<sup>1</sup>*Department of Physics, Harbin Institute of Technology, Harbin 150001, China*

<sup>2</sup>*Institute for Quantum Science and Engineering, and Department of Physics, Southern University of Science and Technology, Shenzhen 518055, China*

<sup>3</sup>*School of Physics, Zhengzhou University, Zhengzhou 450001, China*

(Dated: May 2, 2022)

Nonadiabatic geometric quantum computation (NGQC) has been developed to realize fast and robust geometric gate. However, the previous NGQC is that all of the gates are performed with exactly the same amount of time, whether the geometric rotation angle is large or small, due to the limitation of cyclic condition. Here, we propose an unconventional scheme, called nonadiabatic noncyclic geometric quantum computation (NNGQC), that arbitrary single- and two-qubit geometric gate can be constructed via noncyclic non-Abelian geometric phase. Consequently, this scheme makes it possible to accelerate the implemented geometric gates against the effects from the environmental decoherence. Moreover, our scheme only needs to adjust the amplitude and phase of field in a microwave-coupled or Raman-process-induced resonant two-level system without complex control. Specifically, we consider Rydberg atoms based on the proposed unconventional Rydberg blockade regime for two-qubit gate. After a numerical analysis under same experimental conditions, we found that NNGQC can greatly suppress the decoherence error than NGQC. Therefore, our scheme opens the possibility for fast and robust geometric quantum computation on neutral-atom-based quantum system.

## I. INTRODUCTION

Neutral atoms that interacting via dipole-dipole interactions have became a potential platform for quantum computation [1, 2]. Rydberg atoms are one kind of neutral atoms that are excited to high-lying Rydberg states [3], which would exhibit strong Rydberg dipole-dipole interaction when the inter-atomic distance is not very large. And the Rydberg-Rydberg interaction (RRI) have been studied for construction of quantum logic gates [4–6]. By using microwave transitions, single-qubit Rabi oscillation of neutral atoms have been well studied experimentally [7]. Besides, high fidelity single-qubit quantum logic gates [8–11] and quantum controls [12] have also been demonstrated in neutral atoms. Through the laser-induced transitions from ground state to Rydberg state, many two- and multiple-qubit gates in neutral atom based on Rydebrg-Rydberg-interactions (RRI) have also been demonstrated in experiments [13–20]. These experimental studies show the high-fidelity of single-qubit gates and also show how to improve the fidelity of two-qubit gates step by step. On that basis, if one can design single- and two-qubit quantum logic gates that are more robust to systematic fluctuation error and decoherence, it will be beneficial to realize quantum computation in neutral atoms.

Geometric quantum logic gates [21, 22] based on adiabatic or non-adiabatic geometric phase [23–26], which depends only on the global properties of the evolution paths, provides us the possibility for robust quantum computation [27–33]. In contrast to the earlier adiabatic-process-based geometric quantum computation [34–37], non-adiabatic geometric quantum computation (NGQC) based on Abelian [39–43] and non-Abelian geometric phases [44–52], can intrinsically protect against environment-induced decoherence, since

the the construction times of geometric quantum gates is reduced. The non-adiabatic geometric gates have been experimentally demonstrated in many systems including superconducting qubit [53–58], NMR [59–62], NV center in diamond [63–66]. On the other hand, there are many theoretical proposals to apply geometric quantum computation [67–70] and NGQC [41, 71–74] in Rydberg atom platform. However, NGQC should satisfy the cyclic condition, which leads to Neutral-atom-based quantum logic gates being more sensitive to decay and dephasing errors compared to the conventional dynamical counterparts [8–10]. Specifically, the evolution time of NGQC should be exactly the same for all quantum logic gates no matter the geometric rotation angle is large or small.

Here, we propose an new scheme, nonadiabatic noncyclic geometric quantum computation (NNGQC), that all of single-qubit geometric gate and nontrivial two-qubit can be realized via noncyclic non-Abelian geometric phase in a Rydberg system. Comparing with the conventional Rydberg blockade [4–6], where the dynamical process involving two Rydberg states is always discarded when the RRI strength is much larger than driving laser field Rabi frequency, we consider RRI-induced blockade process seriously by second-order dynamics and employ it to construct the two-qubit logic gate, which may be more accurate since we do not discard the process relevant to the “blockade”. More importantly, our scheme can further reduce the geometric gate time of NGQC [39–43] without the limitation of cyclic condition. Specifically, we found that the certain gate time of NNGQC can be reduced by half compared with NGQC by choosing proper control parameter. Using a numerically thorough analysis on the performance of NNGQC and conventional NGQC under same experimental conditions, the decay and dephasing error caused by the environmental noise can significantly be suppressed via our NNGQC. Furthermore, comparing existing noncyclic schemes [75–77], our scheme only needs to adjust the amplitude and phase of microwave field without complicated pulse

\* [slsu@zzu.edu.cn](mailto:slsu@zzu.edu.cn)

† [yung@sustech.edu.cn](mailto:yung@sustech.edu.cn)

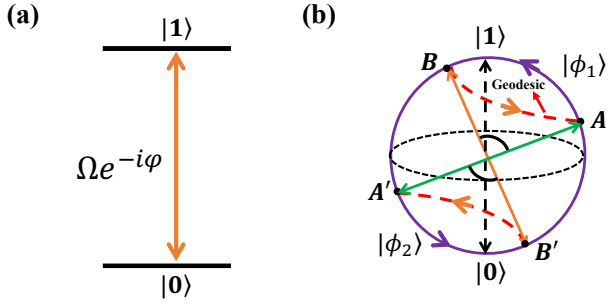


FIG. 1. The illustration of our proposed implementation. (a) The two-level energy structure is resonantly driven by a microwave pulse to realize the transitions of  $|0\rangle \leftrightarrow |1\rangle$  with the Rabi frequency  $\Omega(t)$  and phase  $\varphi(t)$ . (b) Conceptual explanation for noncyclic geometric quantum operation. Noncyclic geometric phase is given by half the area enclosed by the trajectory  $AB(A'B')$  and the geodesic  $BA(B'A')$  connecting the initial and final points.

sequences in a resonant two-level system. Consequently, this easily experimental implementation of NNGQC can be more conveniently applied to various physical platforms such as superconducting qubits and nitrogen-vacancy centers.

## II. THE MODEL AND SINGLE-QUBIT GATE

Here, we consider a  $^{133}\text{Cs}$  with magnetically insensitive “clock” states encoding  $|0\rangle \equiv |6S_{1/2}, F=3, m_F=0\rangle$  and  $|1\rangle \equiv |6S_{1/2}, F=4, m_F=0\rangle$  [79], which is resonantly driven by a microwave pulse to realize the transitions of  $|0\rangle \leftrightarrow |1\rangle$  with the Rabi frequency  $\Omega(t)$  and phase  $\varphi(t)$ , as shown in Fig. 1(a). In the rotating wave approximation and the interaction frame, the system is given by a time-dependent Hamiltonian (here and after  $\hbar \equiv 1$ )

$$H = \frac{1}{2} \begin{pmatrix} 0 & \Omega(t)e^{-i\varphi(t)} \\ \Omega(t)e^{i\varphi(t)} & 0 \end{pmatrix}. \quad (1)$$

For a pair of basis vectors  $\{|\psi_1(t)\rangle, |\psi_2(t)\rangle\}$  following the Schrödinger's equation as  $|\psi_{1,2}(t)\rangle = \mathcal{T}e^{-i\int_0^t H(t')dt'}|\psi_{1,2}(0)\rangle$ , the time-evolution operator can be given by  $U(t, 0) = \mathcal{T}e^{-i\int_0^t H(t')dt'} = |\psi_1(t)\rangle\langle\psi_1(0)| + |\psi_2(t)\rangle\langle\psi_2(0)|$ . Now, we take a set of auxiliary states  $|\phi_1(t)\rangle = (\cos \frac{\chi}{2} e^{-i\frac{\eta}{2}}, \sin \frac{\chi}{2} e^{i\frac{\eta}{2}})^T$  and  $|\phi_2(t)\rangle = (\sin \frac{\chi}{2} e^{-i\frac{\eta}{2}}, -\cos \frac{\chi}{2} e^{i\frac{\eta}{2}})^T$ , with the boundary conditions  $|\phi_m(0)\rangle = |\psi_m(0)\rangle$  at time  $t = 0$ . In this way,  $|\psi_m(t)\rangle$  can be expressed  $|\psi_m(t)\rangle = \sum_l C_{lm}(t) |\phi_l(t)\rangle$ , and the time-evolution operator becomes  $U(t, 0) = \sum_{l,m} C_{lm}(t) |\phi_l(t)\rangle\langle\phi_m(0)|$ . Using the Schrödinger's equation, we obtain the final time evolution operator  $U(\tau, 0) = \sum_{l,m=1}^2 \left( \mathbf{T} e^{i \int_0^\tau (\mathbf{A}(t) + \mathbf{K}(t)) dt} \right)_{lm} |\phi_l(\tau)\rangle\langle\phi_m(0)|$ , with  $\mathbf{A}_{lm} \equiv i \langle\phi_l(t)|(d/dt)|\phi_m(t)\rangle$  being the matrix-valued connection one-form and  $\mathbf{K}_{lm}(t) \equiv -\langle\phi_l(t)|H(t)|\phi_m(t)\rangle$  being dynamical part.

To realize a geometric gate, we choose the auxiliary state  $|\phi_m(t)\rangle$  to be proportional to the dynamical states  $|\psi_m(t)\rangle$ ,

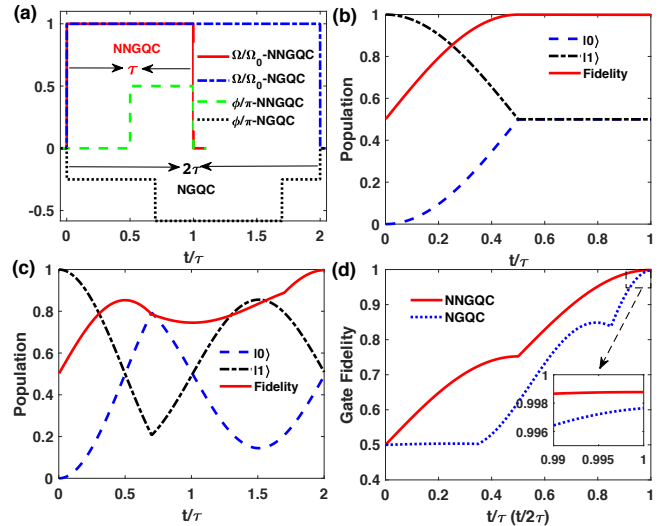


FIG. 2. (a) The Rabi frequency  $\Omega(t)$  and phase  $\varphi(t)$  of  $U_1$  gate for NNGQC and NGQC. State population and state fidelity of (b) NNGQC and (c) NGQC with the initial state being  $\frac{|0\rangle+|1\rangle}{\sqrt{2}}$ . (d) Gate fidelity of  $U_1$  as a function of  $t/\tau$  ( $t/2\tau$ ).

which satisfies the von Neumann equation [46]:  $\frac{d}{dt} \Pi_m(t) = -i [H(t), \Pi_m(t)]$ , where  $\Pi_m(t) \equiv |\phi_m(t)\rangle\langle\phi_m(t)|$  denotes the projector of the auxiliary basis. Explicitly, we found that they are governed by the following coupled differential equations:

$$\Omega(t) = \frac{\dot{\chi}}{\sin(\varphi - \eta)}, \quad \varphi(t) = \eta - \arctan\left(\frac{\dot{\chi}}{\dot{\eta} \tan \chi}\right). \quad (2)$$

In this way, time-evolution operator becomes:

$$U(\tau, 0) = e^{i\gamma} |\phi_1(\tau)\rangle\langle\phi_1(0)| + e^{-i\gamma} |\phi_2(\tau)\rangle\langle\phi_2(0)|, \quad (3)$$

where  $\gamma(\tau) = \int_0^\tau \mathbf{A}_{11} + \mathbf{K}_{11} dt = \int_0^\tau \frac{\dot{\eta}}{\cos \chi} dt$  denotes global phase including the diagonal geometric phase  $\gamma_g = \int_0^\tau \mathbf{A}_{11} dt = \int_0^\tau \frac{1}{2}\dot{\eta} \cos \chi dt$  and diagonal dynamical phase  $\gamma_d = \int_0^\tau \mathbf{K}_{11} dt = -\int_0^\tau \Omega \cos \chi \cos(\varphi - \eta) dt$ . To make evolution gate in Eq. (3) purely geometric, we set  $\varphi - \eta = \pi/2$  for erasing the diagonal dynamical phase. Therefore, the diagonal geometric phase  $\gamma = \int_{\eta(0)}^{\eta(\tau)} \int_{\chi(0)}^{\chi(\tau)} \frac{1}{2} \sin \chi d\chi d\eta = \Omega_{\text{angle}}/2$  is given by half the area enclosed by the trajectory and the geodesic connecting the initial and final points, as shown in Fig. 1(b). Finally, the evolution operator is found to be,

$$U = \begin{bmatrix} e^{-i\eta_-} (X_{\gamma, \chi_+} + iY_{\gamma, \chi_+}) & e^{-i\eta_+} (iZ_{\gamma, \chi_+} - Y_{\chi_-, \gamma}) \\ e^{i\eta_+} (iZ_{\gamma, \chi_+} + Y_{\chi_-, \gamma}) & e^{i\eta_-} (X_{\gamma, \chi_-} + iY_{\gamma, \chi_+}) \end{bmatrix}, \quad (4)$$

where  $X_{a,b} \equiv \cos \frac{a}{2} \cos \frac{b}{2}$ ,  $Y_{a,b} \equiv \sin \frac{a}{2} \cos \frac{b}{2}$ ,  $Z_{a,b} \equiv \sin \frac{a}{2} \sin \frac{b}{2}$ ,  $\chi_\pm = \chi(\tau) - \chi(0)$  and  $\eta_\pm = \eta(\tau) - \eta(0)$ .

To illustrate the geometric rotation,  $U$  is conveniently represented (ignore a global phase) as,

$$U(\theta, \alpha, \beta) = Z_\beta X_\theta Z_\alpha \quad (5)$$

where  $\theta \equiv \sin^{-1}(\sqrt{Z_{\gamma, \chi_+}^2 + Y_{\chi_-, \gamma}^2})$ ,  $\alpha \equiv -\tan^{-1}\left(\frac{Y_{\gamma, \chi_+}}{X_{\gamma, \chi_-}}\right) - \tan^{-1}\left(\frac{Z_{\gamma, \chi_+}}{Y_{\chi_-, \gamma}}\right) + \frac{\eta_- - \eta_+ - \pi}{2}$  and

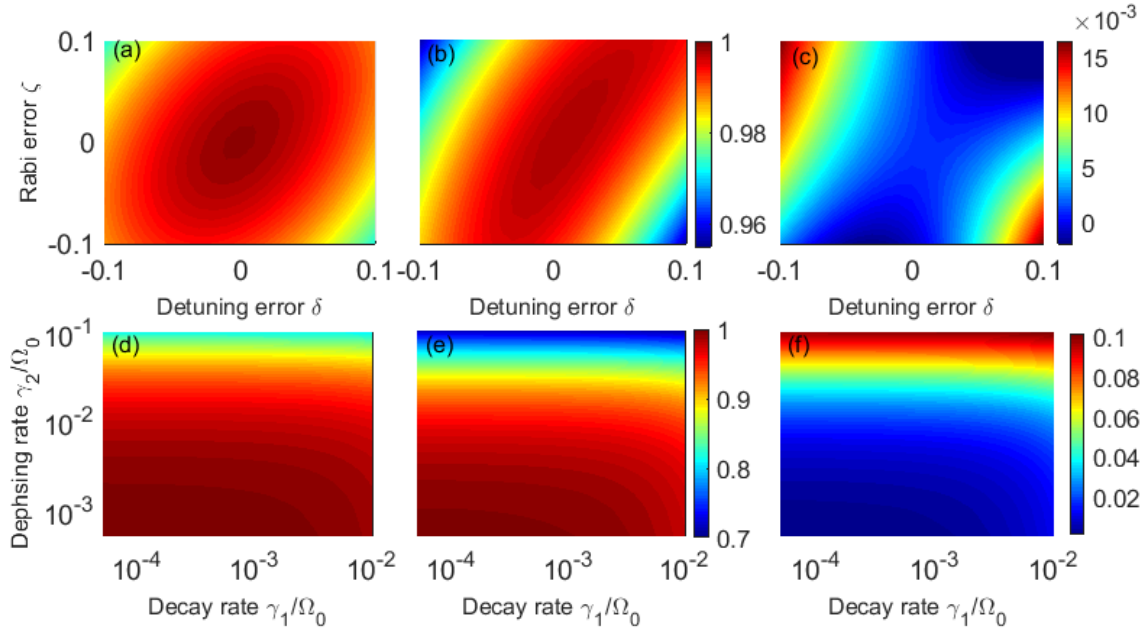


FIG. 3. The performance of  $U_1$  gate under imperfections. Gate fidelities of (a) NNGQC, (b) NGQC under the Rabi error  $\zeta$  and detuning error  $\delta$ . (c) is the difference between (a) and (b). The gate fidelities for (d) NNGQC, (e) NGQC and (f) difference as a function of decay rate  $\gamma_1$  and dephasing rate  $\gamma_2$ , respectively.

$\beta \equiv -\tan^{-1}\left(\frac{Y_{\gamma,x+}}{X_{\gamma,x-}}\right) + \tan^{-1}\left(\frac{Z_{\gamma,x+}}{Y_{x-,\gamma}}\right) + \frac{\eta_- + \eta_+ + \pi}{2}$  are rotation of angles around the  $X$  and  $Z$  axis of the Bloch sphere, respectively. Any single-qubit  $SU(2)$  operation can be realized with  $U(\theta, \alpha, \beta)$  by choosing the geometric phase  $\gamma$ , the initial and final value  $\eta_{\pm}$  and  $\chi_{\pm}$ . For example, we can realize the noncyclic geometric  $U_1 = U(\pi/2, -\pi/2, 0)$  and  $U_2 = U(\pi/2, \pi/2, \pi/2)$  (Hardmard gate) by setting the parameters as  $\{\gamma = \frac{\pi}{2}, \chi_+ = 0, \chi_- = \pi, \eta_{\pm} = \mp\frac{\pi}{2}\}$ , and  $\{\gamma = \frac{\pi}{2}, \chi_+ = -\frac{3\pi}{2}, \chi_- = \frac{\pi}{2}, \eta_{\pm} = \mp\frac{\pi}{2}\}$ , respectively.

To further understand the scheme of our NNGQC, we found that the non-diagonal parts of  $\mathbf{A}$  and  $\mathbf{K}$  satisfy the relations of unconventional quantum holonomy as  $\int_0^\tau \mathbf{A}_{km} dt = -\int_0^\tau \mathbf{K}_{km} dt = -\frac{1}{2} \int_0^\tau \Omega [\cos \chi \cos(\phi - \eta) - i \sin(\phi - \eta)] dt$  for  $k \neq m$ . Although  $\mathbf{A} + \mathbf{K}$  is a diagonal matrix,  $\mathbf{A}$  and  $\mathbf{K}$  are both non-diagonal in our scheme. Specifically,  $\mathbf{A}$  does represent a non-abelian connection with non-vanishing commutation relation  $[\mathbf{A}(t), \mathbf{A}(t')] \neq 0$ , which proves the non-Abelian nature of the gate in Eq. (4) [26].

Note that the key difference between the previous NGQC schemes and the non-cyclic approach introduced here is whether to meet the cyclic conditions  $\eta_- = 0$  and  $\chi_- = 0$ . In the previous NGQC based on cyclic geometric phase, all of the operations are performed with exactly the same amount of time, even for a small-angle rotation. However, for our method, NNGQC removes the constraints, which makes it possible to accelerate the implemented geometric gates against decoherence by picking the variables  $\eta(t)$  and  $\chi(t)$ .

Now, to construct the NNGQC gate, one simple parameter set of choice is found to be,

$$\chi(t) = \Omega_0 t - \chi_0, \quad \eta(t) = \phi_1 \epsilon(t) + \phi_0 \quad (6)$$

where the step function  $\epsilon(t)$  satisfies  $\epsilon = 0$  with  $t \in [0, \frac{\chi_0}{\Omega_0}]$  and  $\epsilon = 1$  with  $t \in [\frac{\chi_0}{\Omega_0}, \tau]$  and  $\Omega_0, \phi_1, \phi_0$  and  $\chi_0$  are constants. With the settings, we can obtain the initial and final value  $\eta_{\pm}$  and  $\chi_{\pm}$  as  $\eta_+ = 2\phi_1 + \phi_0, \eta_- = \phi_0, \chi_+ = \Omega_0\tau - 2\chi_0, \chi_- = \Omega_0\tau$ . Meanwhile, the geometric phase is taken by

$$\gamma = \phi_1 - \phi_0. \quad (7)$$

For  $U_1$  gate, the control parameters are chosen as  $\chi_0 = -\pi/2, \phi_0 = 0, \phi_1 = \pi/2$ , and  $\tau = \frac{\pi}{\Omega_0}$ . Comparing with conventional NGQC [41–43, 56, 58], we found that the  $U_1$  gate time of NNGQC ( $\tau$ ) can be reduced by 50% compared with NGQC ( $2\tau$ ) by choosing the same maximum Rabi frequency, as shown in Fig. 2(a).

### III. GATE PERFORMANCE OF NNGQC

The performance of the  $U_1$  gate can be simulated by using a master equation in the Lindblad form [78] as,

$$\dot{\rho}(t) = i[\rho(t), H(t)] + \frac{1}{2} [\gamma_1 \mathcal{L}(\sigma^+) + \gamma_2 \mathcal{L}(\sigma_z)], \quad (8)$$

where  $\rho(t)$  is the density matrix of the considered system and  $\mathcal{L}(A) = 2A\rho_1 A^\dagger - A^\dagger A\rho_1 - \rho_1 A^\dagger A$  is the Lindbladian of the operator  $A$ ,  $\sigma^+ = |0\rangle\langle 1|$ , and  $\sigma_z = |0\rangle\langle 0| - |1\rangle\langle 1|$ . In addition  $\gamma_1$  and  $\gamma_2$  are the decay and dephasing rates of the single-qubit system, respectively. In our simulation, we have used the following set of experimental parameter [8–10]. The Rabi frequency, decay and dephasing rates are set as  $\Omega_0 = 2\pi \times 6.25$  kHz,  $\gamma_1 \approx 2\Omega_0 \times 10^{-4}$  Hz and

$\gamma_2 \approx 2\Omega_0 \times 10^{-3}$  Hz corresponding to  $T_1 = 590\text{ms}$  and  $T_2 = 50\text{ms}$ . Suppose that the qubit is initially prepared in the  $|\psi(0)\rangle = \frac{1}{\sqrt{2}}(|0\rangle + |1\rangle)$  state, the time-dependence of the state populations and the state fidelity  $F = |\langle\psi_I|\psi(\tau)\rangle|^2$  of realizing the  $U_1$  gate for NNGQC and NGQC are depicted in Fig. 2(b) and 2(c), where the state fidelities of NNGQC and NGQC are obtained to be 99.87% and 99.75%, respectively. Furthermore, we have also investigated the gate fidelity of  $U_1$  defined by  $F = (1/2\pi) \int_0^{2\pi} \langle\psi_I|\rho|\psi_I\rangle d\Theta$  for initial states of the form  $|\psi\rangle = \cos\Theta|0\rangle + \sin\Theta|1\rangle$ , where a total of 1001 different values of  $\Theta$  were uniformly chosen in the range of  $[0, 2\pi]$ , as shown in Fig. 2(d). We found that the gate error (1-F) of NNGQC can be reduced by as much as 50% compared with the gate error of NGQC (0.24%).

Now, we start to demonstrate the robustness of our scheme. We firstly consider the robustness of our NNGQC against Rabi errors and assume the amplitudes of control pulse to vary in the range of  $\Omega_0 \rightarrow (1 + \zeta)\Omega_0$  with the error fraction  $\zeta \in [-0.1, 0.1]$ . Next, we take the detuning noise to be  $\Delta\sigma_z$  with  $\Delta = \delta\Omega_0$  being static and the fraction is  $\delta \in [-0.1, 0.1]$ . Comparing our NNGQC with the conventional NGQC methods, we plot the performance of the same geometric gate with the same pulse error. As shown in Fig. 3(a), Fig. 3(b) and Fig. 3(c), the NNGQC is always more robust than the NGQC gate. Furthermore, we also simulated the gate fidelity as a function of decay rate and dephasing rate  $\gamma_1$  and  $\gamma_2$ . For above two schemes as shown in Fig. 3(d), Fig. 3(e) and Fig. 3(f), our scheme of NNGQC can greatly suppress the decoherence effect comparing with the conventional NGQC.

#### IV. NONTRIVIAL TWO-QUBIT RYDBERG GEOMETIRC GATE WITH UNCONVENTIONAL RYDBERG BLOCKADE

In this section, we proceed to implement nontrivial two-qubit Rydberg quantum gates free from blockade error with the pulse similar to that designed in Sec. II. As shown in Fig. 4, we consider two  $^{133}\text{Cs}$  atoms with magnetically insensitive ‘‘clock’’ states encoding  $|0\rangle \equiv |6S_{1/2}, F = 3, m_F = 0\rangle$  and  $|1\rangle \equiv |6S_{1/2}, F = 4, m_F = 0\rangle$  [79]. The Rydberg state is chosen as  $|R\rangle \equiv |61S_{1/2}\rangle$ . And the  $C_6$  parameters can be evaluated as 126 GHz· $\mu\text{m}^6$  [80].

To construct the seminal two-qubit quantum logic gates [4, 5] or the high-fidelity two-qubit quantum logic [81] via two-atom dark state, three steps are required. Here we follow the basic steps. However, the present scheme would show high robustness and high-fidelity by the virtue of method of noncyclic nonadiabatic geometric operation and the unconventional Rydberg blockade model.

The basic process of two-qubit gate is shown in Fig. 4, where the control in resonant interaction but the target atom is large-detuning interaction. The required three steps are as follows.

*Step (i).* Turn on the laser on control atom with Hamiltonian

$$H_c = \frac{\Omega_1(t)}{2} |1\rangle\langle R| + \text{H.c.}, \quad (9)$$

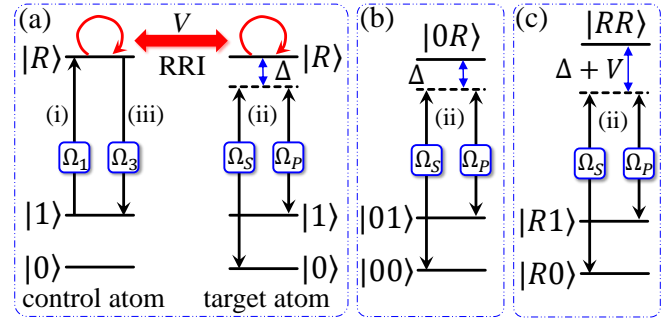


FIG. 4. (a) Illustration of the two-qubit quantum controlled gate based on unconventional Rydberg blockade with single-atom basis.  $|0\rangle$  and  $|1\rangle$  are two ground states to encode quantum information.  $|R\rangle$  denotes the Rydberg state. For control atom,  $|1\rangle$  is coupled with  $|R\rangle$  through two-photon process with Rabi frequency  $\Omega_1$  ( $\Omega_3$ ) in step (i) [(iii)]. For target atom,  $|0\rangle$  ( $|1\rangle$ ) is coupled with  $|R\rangle$  with Rabi frequency  $\Omega_S$  ( $\Omega_P$ ) and detuning  $\Delta$  via two-photon process in step (ii).  $\Omega_j = |\Omega_j|e^{i\varphi_j}$  with  $j = 1, 3, S, P$ . (b) Dynamical process of step (ii) under two-atom basis in the absence of RRI. (c) Dynamical process of step (ii) under two-atom basis in the case without RRI. For conventional blockade, the dynamical process in (b) is resonant while in (c) is detuned by  $V$  and the dynamical process is always ignored when the large detuning condition  $V \gg \Omega_{S(P)}$  is satisfied, which is known as ‘‘Rydberg blockade’’. However, in our scheme, both of the dynamical processes in (b) and (c) are used for the construction of the gate, we thus call it ‘‘unconventional Rydberg blockade’’. In our scheme, the dynamical process may be more accurate in contrast to the conventional Rydberg blockade since we do not ignore the process induced by RRI-induced ‘‘blockade’’ terms.

where  $\Omega_1(t) \equiv |\Omega_1(t)|e^{i\varphi_1(t)}$ . We set  $\varphi_1(t) = 0$  and  $\int \Omega_1(t)dt = \pi$  in step (i).

*Step (ii).* Turn off the laser on control atom and turn on lasers with Rabi frequencies  $\Omega_S$  and  $\Omega_P$  on target atom. The Hamiltonian is

$$H_t = \Delta|R\rangle\langle R| + \frac{1}{2} \left[ \Omega_S(t)|0\rangle + \Omega_P(t)|1\rangle \right] \langle R| + \text{H.c.}, \quad (10)$$

where  $\Omega_S(t) \equiv |\Omega_S(t)|e^{i\varphi_S(t)}$  and  $\Omega_P(t) \equiv |\Omega_P(t)|e^{i\varphi_P(t)}$ . Besides, the RRI Hamiltonian

$$H_V = V|RR\rangle\langle RR| \quad (11)$$

may be in existence conditioned on the control atom is excited or not. We use  $|mn\rangle\langle mn|$  to denote the abbreviation of  $|m\rangle\langle m| \otimes |n\rangle\langle n|$  here and throughout the manuscript for simplify. Thus, the dynamical process can be classified as two cases in Fig. 4(b) and Fig. 4(c), respectively, depend whether the control atom is not excited or excited.

The effective Hamiltonian in Fig. 4(b) can be calculated as

$$H_{\text{eff},1} = \frac{\Omega_{\text{eff},1}}{2} |00\rangle\langle 01| + \text{H.c.}, \quad (12)$$

where  $\Omega_{\text{eff},1} = \Omega_S\Omega_P^*/(2\Delta)$  and the stark shifts are vanished when  $|\Omega_S| = |\Omega_P|$ . Similarly, the effective Hamiltonian in Fig. 4(c) would be

$$H_{\text{eff},2} = \frac{\Omega_{\text{eff},2}}{2} |R0\rangle\langle R1| + \text{H.c.}, \quad (13)$$

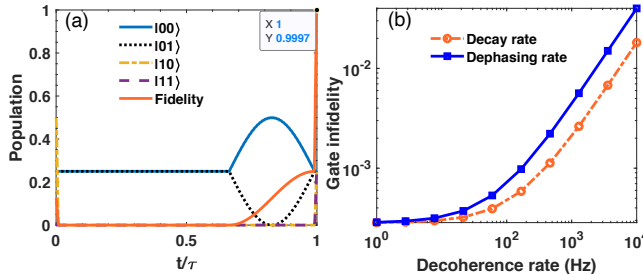


FIG. 5. (a) State population and state fidelity of two-qubit gate in Eq. (16) with the initial state being  $\frac{1}{2}(|00\rangle + |01\rangle + \sqrt{2}|10\rangle)$ . (b) Gate infidelity as a function of decay rate and dephasing rate for Rydberg state .

where  $\Omega_{\text{eff},2} = \Omega_S \Omega_P^* / [2(\Delta + V)]$  and the stark shifts are vanished when  $|\Omega_S| = |\Omega_P|$ .

Equations (12) and (13) have similar form as Eq. (1). Thus, we can use the similar pulses to construct the noncyclic nonadiabatic geometric operations. That is, in step (ii), one can get the operation

$$\mathcal{U}_2 = |0\rangle_c \langle 0| \otimes U(\theta_1, \alpha_1, \beta_1) + |R\rangle_c \langle R| \otimes U(\theta_2, \alpha_2, \beta_2) \quad (14)$$

with suitable laser parameters.

*Step(iii).* Turn off the lasers on target atom and at the same time turn on laser with Rabi frequency  $\Omega_3(t)$  on control atom. If  $|\Omega_3(t - t_2)| = |\Omega_1(t)|$  and  $\varphi_3 = \pi$ , in which  $t_2$  denotes the evolution time in step (ii), one can get the the whole evolution operator as

$$\mathcal{U} = |0\rangle_c \langle 0| \otimes U(\theta_1, \alpha_1, \beta_1) + |1\rangle_c \langle 1| \otimes U(\theta_2, \alpha_2, \beta_2). \quad (15)$$

Therefore, in general, we know that Eq. (15) represents a nontrivial two-qubit entangled gate, since  $U$  in subspace  $\{|00\rangle, |01\rangle\}$  and  $\{|10\rangle, |11\rangle\}$  is different.

When  $\theta_1 = \pi/2, \alpha_1 = \pi/2, \beta_1 = \pi/2$  and  $\Delta = V$ , we obtain two-qubit entangled gate with matrix representation as

$$\mathcal{U} = \begin{pmatrix} 0 & i & 0 & 0 \\ -i & 0 & 0 & 0 \\ 0 & 0 & \frac{e^{i\pi/4}}{\sqrt{2}} & \frac{e^{i\pi/4}}{\sqrt{2}} \\ 0 & 0 & \frac{e^{i\pi/4}}{\sqrt{2}} & \frac{-e^{i\pi/4}}{\sqrt{2}} \end{pmatrix}. \quad (16)$$

To evaluate the performance of two-qubit entangled gate, we take the parameters from the state-of-art experiments as the Rabi frequency  $\Omega_0 = \Omega_1 = 2\pi \times 10$  MHz and the detuning  $\Delta \approx 17\Omega_0$ , where  $\Omega_P$  and  $\Omega_S$  are governed by the Eq. (6). As shown in Fig.5(a), we plot the state populations and the state fidelity of the two-qubit gate with the initial state  $|\psi(0)\rangle = \frac{1}{2}(|00\rangle + |01\rangle + \sqrt{2}|10\rangle)$ , where the state fidelity is

obtained to be 99.97% without considering relaxation. Moreover, we have also investigated the gate infidelity [82, 83] of two-qubit  $1 - F$  as a function of decay rate and dephasing rate of Rydberg state as shown in Fig. 5(b), and found that our two-qubit geometric gate is robust against decoherence from the environmental noises.

One of the practical applications of the two-qubit logic gate is to prepare the Knill-Laflamme-Milburn (KLM)-like entangled state [84]  $|\Psi\rangle = (|00\rangle - |01\rangle + e^{-i\pi/4}|10\rangle)/\sqrt{2}$  directly by performing  $\mathcal{U}$  on the kronecker product state of two atoms  $|\Psi(0)\rangle = (|0\rangle + |1\rangle)/\sqrt{2} \otimes (|0\rangle + |1\rangle)/\sqrt{2}$ . More generally, on the premise that the the conditions  $\Delta \gg \Omega$  and  $\Delta + V \gg \Omega$  are fulfilled, one can change the values of  $\Delta$  by modulating laser frequency and of  $V$  by setting the inter-atomic distance to achieve the other universal two-qubit logic gates.

## V. CONCLUSION

In summary, we have presented a new framework, called NNGQC, which universal nonadiabatic geometric gates can be constructed via noncyclic non-Abelian geometric phase. Comparing with conventional NGQC, NNGQC can further reduce the geometric gate time beyond the limitation of cyclic condition. Consequently, our proposal is more robust against the decay and dephasing effects from the environmental decoherence. Moreover, we also presented an explicit way to implement our scheme using a resonate two-level system, and numerically simulated the performance of pulse optimization for Rydberg atom platform, where the gate fidelity can be significantly improved than conventional geometric method. Furthermore, we construct a nontrivial two-qubit geometric gate via RRI-induced large detuning process seriously without ignoring the process induced by RRI-induced “blockade” terms. Therefore, our scheme provides a promising way towards fault-tolerant quantum computation for neutral-atom-based quantum system.

## ACKNOWLEDGMENTS

This work is supported by the Key-Area Research and Development Program of Guangdong Province (Grant No.2018B030326001), the National Natural Science Foundation of China (Grant No.11875160, No.11874156 and No.11804308), the Natural Science Foundation of Guangdong Province (Grant No.2017B030308003), the National Key R & D Program of China (Grant No.2016YFA0301803, the Guangdong Innovative and Entrepreneurial Research Team Program (Grant No.2016ZT06D348), the Economy, Trade and Information Commission of Shenzhen Municipality (Grant No.201901161512), the Science, Technology and Innovation Commission of Shenzhen Municipality (Grant No. JCYJ20170412152620376, No. JCYJ20170817105046702, and No. KYTDPT20181011104202253).

---

[1] G. K. Brennen, C. M. Caves, P. S. Jessen, and I. H. Deutsch, "Quantum Logic Gates in Optical Lattices," *Phys. Rev. Lett.* **82**, 1060 (1999).

[2] D. S. Weiss and M. Saffman, "Quantum computing with neutral atoms," *Phys. Today* **70**, 44 (2017).

[3] T. F. Gallagher, "Rydberg Atoms" (Cambridge University Press, Cambridge, UK, 1994).

[4] D. Jaksch, J. I. Cirac, P. Zoller, S. L. Rolston, R. Ct, and M. D. Lukin, "Fast Quantum Gates for Neutral Atoms," *Phys. Rev. Lett.* **85**, 2208 (2000).

[5] M. D. Lukin, M. Fleischhauer, R. Ct, L. M. Duan, D. Jaksch, J. I. Cirac, and P. Zoller, "Dipole Blockade and Quantum Information Processing in Mesoscopic Atomic Ensembles," *Phys. Rev. Lett.* **87**, 037901 (2001).

[6] M. Saffman, T. G. Walker, and K. Mølmer, "Quantum information with Rydberg atoms," *Rev. Mod. Phys.* **82**, 2313 (2010).

[7] D. Schrader, I. Dotsenko, M. Khudaverdyan, Y. Miroshnychenko, A. Rauschenbeutel, and D. Meschede, "Neutral Atom Quantum Register," *Phys. Rev. Lett.* **93**, 150501 (2004).

[8] S. Olmschenk, R. Chicireanu, K. D. Nelson, and J. V. Porto, "Randomized benchmarking of atomic qubits in an optical lattice," *New J. Phys.* **12**, 113007 (2010).

[9] T. Xia, M. Lichtman, K. Maller, A.W. Carr, M. J. Piotrowicz, L. Isenhower, and M. Saffman, "Randomized Benchmarking of Single-Qubit Gates in a 2D Array of Neutral-Atom Qubits," *Phys. Rev. Lett.* **114**, 100503 (2015).

[10] Y. Wang, X. Zhang, T. A. Corcovilos, A. Kumar, and D.S. Weiss, "Coherent Addressing of Individual Neutral Atoms in a 3D Optical Lattice," *Phys. Rev. Lett.* **115**, 043003 (2015). Yang Wang, Aishwarya Kumar, Tsung-Yao Wu, David S. Weiss, "Single-qubit gates based on targeted phase shifts in a 3D neutral atom array," *Science* **352**, 1562 (2016).

[11] J.H. Lee, E. Montano, I.H. Deutsch, P.S. Jessen, "Robust site-resolvable quantum gates in an optical lattice via inhomogeneous control," *Nat. Commun.* **4** 2027 (2013).

[12] A. Smith, B. E. Anderson, H. Sosa-Martinez, C. A. Riofrío, Ivan H. Deutsch, and Poul S. Jessen, "Quantum Control in the Cs  $6S_{1/2}$  Ground Manifold Using Radio-Frequency and Microwave Magnetic Fields," *Phys. Rev. Lett.* **111**, 170502 (2013).

[13] L. Isenhower, E. Urban, X. L. Zhang, A. T. Gill, T. Henage, T. A. Johnson, T. G. Walker, and M. Saffman, "Demonstration of a Neutral Atom Controlled-NOT Quantum Gate," *Phys. Rev. Lett.* **104**, 010503 (2010).

[14] T. Wilk, A. Gaëtan, C. Evellin, J. Wolters, Y. Miroshnychenko, P. Grangier, and A. Browaeys, "Entanglement of Two Individual Neutral Atoms Using Rydberg Blockade," *Phys. Rev. Lett.* **104**, 010502 (2010).

[15] K. M. Maller, M. T. Lichtman, T. Xia, Y. Sun, M. J. Piotrowicz, A. W. Carr, L. Isenhower, and M. Saffman, "Rydberg-blockade controlled-not gate and entanglement in a two-dimensional array of neutral-atom qubits," *Phys. Rev. A* **92**, 022336 (2015).

[16] Y. Zeng, P. Xu, X. He, Y. Liu, M. Liu, J. Wang, D. J. Papoulier, G. V. Shlyapnikov, and M. Zhan, "Entangling Two Individual Atoms of Different Isotopes via Rydberg Blockade," *Phys. Rev. Lett.* **119**, 160502 (2017).

[17] C. J. Picken, R. Legaie, K. McDonnell, and J. D. Pritchard, "Entanglement of neutral-atom qubits with long ground-Rydberg coherence times," *Quan. Sci. Tech.* **4**, 015011 (2018).

[18] H. Levine, A. Keesling, A. Omran, H. Bernien, S. Schwartz, A. S. Zibrov, M. Endres, M. Greiner, V. Vuletić, and M. D. Lukin, "High-Fidelity Control and Entanglement of Rydberg-Atom Qubits," *Phys. Rev. Lett.* **121**, 123603 (2018).

[19] H. Levine, A. Keesling, G. Semeghini, A. Omran, T. T. Wang, S. Ebadi, H. Bernien, M. Greiner, V. Vuletić, H. Pichler, and M. D. Lukin, "Parallel Implementation of High-Fidelity Multi-qubit Gates with Neutral Atoms," *Phys. Rev. Lett.* **123**, 170503 (2019).

[20] T. M. Graham, M. Kwon, B. Grinkemeyer, Z. Marra, X. Jiang, M. T. Lichtman, Y. Sun, M. Ebert, and M. Saffman, "Rydberg mediated entanglement in a two-dimensional neutral atom qubit array," *Phys. Rev. Lett.* **123**, 230501 (2019).

[21] E. Sjöqvist, "Trend: A new phase in quantum computation," *Physics* **1**, 35 (2008). E. Sjöqvist, "Geometric phases in quantum information," *Int. J. Quantum Chem.* **115**, 1311 (2015).

[22] P. Zanardi, and M. Rasetti, "Holonomic quantum computation," *Phys. Lett. A* **264**, 94 (1999); J. Pachos, P. Zanardi, and M. Rasetti, *Phys. Rev. A* **61**, 010305(R) (1999).

[23] M. V. Berry, "Quantal phase factors accompanying adiabatic changes," *Proc. R. Soc. Lond. A* **392**, 45 (1984).

[24] F. Wilczek, and A. Zee, "Appearance of gauge structure in simple dynamical systems," *Phys. Rev. Lett.* **52**, 2111 (1984).

[25] Y. Aharonov, and J. Anandan, "Phase change during a cyclic quantum evolution," *Phys. Rev. Lett.* **58**, 1593 (1987).

[26] J. Anandan, "Non-adiabatic non-abelian geometric phase," *Phys. Lett. A* **133**, 171 (1988).

[27] S.-L. Zhu, and P. Zanardi, "Geometric quantum gates that are robust against stochastic control errors," *Phys. Rev. A* **72**, 020301(R) (2005).

[28] S. Berger, M. Pechal, A. A. Abdumalikov, Jr. C. Eichler, L. Steffen, A. Fedorov, A. Wallraff, and S. Filipp, "Exploring the effect of noise on the Berry phase," *Phys. Rev. A* **87**, 060303(R) (2013).

[29] G. D. Chiara and G. M. Palma, "Berry phase for a spin-1/2 particle in a classical fluctuating field," *Phys. Rev. Lett.* **91**, 090404 (2003).

[30] P. J. Leek, J. M. Fink, A. Blais, R. Bianchetti, M. Gppi, J. M. Gambetta, D. I. Schuster, L. Frunzio, R. J. Schoelkopf, and A. Wallraff, "Observation of Berry's phase in a solid state qubit," *Science* **318**, 1889 (2007).

[31] S. Filipp, J. Klepp, Y. Hasegawa, C. Plonka-Spehr, U. Schmidt, P. Geltenbort, and H. Rauch, "Experimental demonstration of the stability of Berry's phase for a spin-1/2 particle," *Phys. Rev. Lett.* **102**, 030404 (2009).

[32] J. T. Thomas, M. Lababidi, and M. Tian, "Robustness of single-qubit geometric gate against systematic error," *Phys. Rev. A* **84**, 042335 (2011).

[33] M. Johansson, E. Sjöqvist, L. M. Andersson, M. Ericsson, B. Hessmo, K. Singh, and D. M. Tong, "Robustness of non-adiabatic holonomic gates," *Phys. Rev. A* **86**, 062322 (2012).

[34] L. M. Duan, J. I. Cirac, and P. Zoller, "Geometric Manipulation of Trapped Ions for Quantum Computation," *Science* **292**, 1695 (2001).

[35] L.-A. Wu, P. Zanardi, and D. A. Lidar, "Holonomic Quantum Computation in Decoherence-Free Subspaces," *Phys. Rev. Lett.* **95**, 130501 (2005).

[36] J. A. Jones, V. Vedral, A. Ekert, and G. Castagnoli, "Geometric quantum computation using nuclear magnetic resonance," *Nature* **403**, 869 (2000).

[37] Y.-Y. Huang, Y.-K. Wu, F. Wang, P.-Y. Hou, W.-B. Wang, W.-G. Zhang, W.-Q. Lian, Y.-Q. Liu, H.-Y. Wang, H.-Y. Zhang, et al., "Experimental Realization of Robust Geometric Quantum Gates with Solid-State Spins," *Phys. Rev. Lett.* **122**, 010503 (2019).

[38] Wang, X. B., and M. Keiji, Nonadiabatic conditional geometric phase shift with NMR," Phys. Rev. Lett. **87**, 097901 (2001).

[39] S.-L. Zhu, and Z. D. Wang, Implementation of universal quantum gates based on nonadiabatic geometric phases," Phys. Rev. Lett. **89**, 097902 (2002).

[40] Z.-T. Liang, X. Yue, Q. Lv, Y.-X. Du, W. Huang, H. Yan, and S.-L. Zhu, Proposal for implementing universal superadiabatic geometric quantum gates in nitrogen-vacancy centers," Phys. Rev. A **93** 040305(R) (2016).

[41] P. Z. Zhao, X.-D. Cui, G. F. Xu, E. Sjöqvist, and D. M. Tong, Rydberg-atom-based scheme of nonadiabatic geometric quantum computation," Phys. Rev. A **96**, 052316 (2017).

[42] T. Chen and Z.-Y. Xue, Nonadiabatic geometric quantum computation with parametrically tunable coupling," Phys. Rev. Appl. **10**, 054051 (2018).

[43] C. Zhang, T. Chen, S. Li and Z.-Y. Xue, High-fidelity geometric gate for silicon-based spin qubits," Phys. Rev. A **101**, 052302 (2020).

[44] E. Sjöqvist, D. M. Tong, L. M. Andersson, B. Hessmo, M. Johansson, and K. Singh1, Non-adiabatic holonomic quantum computation," New J. Phys. **14**, 103035 (2012).

[45] G. F. Xu, J. Zhang, D. M. Tong, E. Sjöqvist, and L. C. Kwek, Nonadiabatic Holonomic Quantum Computation in Decoherence-free Subspaces," Phys. Rev. Lett.**109**, 170501 (2012).

[46] B.-J. Liu, X.-K. Song, Z.-Y. Xue, X. Wang, and M.-H. Yung, Plug-and-Play Approach to Nonadiabatic Geometric Quantum Gates," Phys. Rev. Lett., **123** 100501 (2019).

[47] B.-J. Liu, Z.-Y. Xue, and M.-H. Yung, Brachistochronic Non-Adiabatic Holonomic Quantum Control," [arXiv:2001.05182](https://arxiv.org/abs/2001.05182) (2020).

[48] Z.-Y. Xue, F.-L. Gu, Z.-P. Hong, Z.-H. Yang, D.-W. Zhang, Y. Hu, and J. Q. You, Nonadiabatic holonomic quantum computation with dressed-state qubits," Phys. Rev. Appl. **7**, 054022 (2017).

[49] V. Azimi Mousolou, Electric nonadiabatic geometric entangling gates on spin qubits," Phys. Rev. A **96**, 012307 (2017).

[50] X.-K. Song, H. Zhang, Q. Ai, J. Qiu, and F.-G. Deng, Shortcuts to adiabatic holonomic quantum computation in decoherence-free subspace with transitionless quantum driving algorithm," New J. Phys. **18**, 023001 (2016).

[51] B.-J. Liu, Z.-H. Huang, Z.-Y. Xue, and X.-D. Zhang, Superadiabatic holonomic quantum computation in cavity QED," Phys. Rev. A **95**, 062308 (2017).

[52] Y.-H. Kang, Z.-C. Shi, B.-H. Huang, J. Song, and Y. Xia, Flexible scheme for the implementation of nonadiabatic geometric quantum computation," Phys. Rev. A **101**, 032322 (2020).

[53] A. A. Abdumalikov, J. M. Fink, K. Jullusson, M. Pechal, S. Berger, A. Wallraff, and S. Filipp, Experimental realization of non-Abelian non-adiabatic geometric gates, Nature **496**, 482-485 (2013).

[54] C. Song, S.-B. Zheng, P. Zhang, K. Xu, L. Zhang, Q. Guo, W. Liu, D. Xu, H. Deng, K. Huang, *et al.*, Continuous-variable geometric phase and its manipulation for quantum computation in a superconducting circuit, Nat. Commun. **8**, 1061 (2017).

[55] T. Yan *et al*, Experimental Realization of non-Adiabatic Shortcut to non-Abelian Geometric Gates, Phys. Rev. Lett. **122**, 080501 (2019).

[56] Y. Xu *et al*, Single-Loop Realization of Arbitrary Nonadiabatic Holonomic Single-Qubit Quantum Gates in a Superconducting Circuit, Phys. Rev. Lett. **121**, 110501 (2018). Y. Xu *et al*, Experimental implementation of universal nonadiabatic geometric quantum gates in a superconducting circuit, [arXiv:1910.12271](https://arxiv.org/abs/1910.12271).

[57] Z. Han *et al*, Experimental Realization of Universal Time-optimal non-Abelian Geometric Gates, arXiv:2004.10364.

[58] P. Z. Zhao, Z. Dong, Z. Zhang, G. Guo, D. M. Tong, and Y. Yin, Experimental realization of nonadiabatic geometric gates with a superconducting xmon qubit, arXiv , 1909.09970 (2019).

[59] G. Feng, G. Xu, and G. Long, Experimental Realization of Nonadiabatic Holonomic Quantum Computation, Phys. Rev. Lett. **110**, 190501(2013).

[60] H. Li, L. Yang, and G. Long, Experimental realization of single-shot nonadiabatic holonomic gates in nuclear spins, Sci. China: Phys., Mech. Astron. **60**, 080311(2017).

[61] Z. Zhu, T. Chen, X. Yang, J. Bian, Z.-Y. Xue, and X. Peng, Single-Loop and Composite-Loop Realization of Nonadiabatic Holonomic Quantum Gates in a Decoherence-Free Subspace, Phys. Rev. Appl. **12**, 024024 (2019).

[62] Y. Li, T. Xin, C. Qiu, K. Li, G. Liu, J. Li, Y. Wan, and D. Lu, Dynamical-Invariant-based Holonomic Quantum Gates: Theory and Experiment, [arXiv:2003.09848](https://arxiv.org/abs/2003.09848).

[63] C. Zu *et al*, Experimental realization of universal geometric quantum gates with solid-state spins, Nature (London) **514**, 72 (2014).

[64] S. Arroyo-Camejo, A. Lazariev, S. W. Hell, and G. Balasubramanian, Room temperature high-fidelity holonomic single-qubit gate on a solid-state spin, Nat. Commun. **5**, 4870 (2014).

[65] Y. Sekiguchi, N. Niikura, R. Kuroiwa, H. Kano, and H. Kosaka, Optical holonomic single quantum gates with a geometric spin under a zero field, Nat. Photonics **11**, 309 (2017).

[66] B. B. Zhou, P. C. Jerger, V. O. Shkolnikov, F. Joseph Heremans, G. Burkard, and D. D. Awschalom, Holonomic Quantum Control by Coherent Optical Excitation in Diamond, Phys. Rev. Lett. **119**, 140503 (2017)

[67] D. Møller, L. B. Madsen, and K. Mølmer, Quantum Gates and Multiparticle Entanglement by Rydberg Excitation Blockade and Adiabatic Passage, Phys. Rev. Lett. **100**, 170504 (2008).

[68] Y.-C. Zheng and T. A. Brun, Geometric manipulation of ensembles of atoms on an atom chip for quantum computation, Phys. Rev. A **86**, 032323 (2012).

[69] I. I. Beterov, M. Saffman, E. A. Yakshina, V. P. Zhukov, D. B. Tretyakov, V. M. Entin, I. I. Ryabtsev, C. W. Mansell, C. McCormick, S. Bergamini, and M. P. Fedoruk, Quantum gates in mesoscopic atomic ensembles based on adiabatic passage and Rydberg blockade, Phys. Rev. A **88**, 010303 (2013).

[70] H. Wu, X.-R. Huang, C.-S. Hu, Z.-B. Yang, and S.-B. Zheng, Rydberg-interaction gates via adiabatic passage and phase control of driving fields, Phys. Rev. A **96**, 022321 (2017).

[71] P. Z. Zhao, X. Wu, T. H. Xing, G. F. Xu, and D. M. Tong, Nonadiabatic holonomic quantum computation with Rydberg superatoms, Phys. Rev. A **98**, 032313 (2018).

[72] Y.-H. Kang, Y.-H. Chen, Z.-C. Shi, B.-H. Huang, J. Song, and Y. Xia, Nonadiabatic holonomic quantum computation using Rydberg blockade," Phys. Rev. A **97**, 042336 (2018).

[73] C.-P. Shen, J.-L. Wu, S.-L. Su, and E. Liang, Construction of robust Rydberg controlled-phase gates," Opt. Lett. **44**, 2036 (2019).

[74] K.-Y. Liao, X.-H. Liu, Z. Li, and Y.-X. Du, Geometric Rydberg quantum gate with shortcuts to adiabaticity," Opt. Lett. **44**, 4801 (2019).

[75] A. Friedenauer and E. Sjöqvist, Noncyclic geometric quantum computation," Phys. Rev. A **67**, 024303 (2003).

[76] Q.-X. Lv, Z.-T. Liang, H.-Z. Liu, J.-H. Liang, K.-Y. Liao, and Y.-X. Du, Noncyclic geometric quantum computation with shortcut to adiabaticity," Phys. Rev. A **101**, 022330 (2020).

[77] T. Wang *et al*, The experimental realization of high-fidelity shortcut-to-adiabaticity quantum gates in a superconducting

Xmon qubit,” *New J. Phys.* **20**, 065003 (2018).

[78] G. Lindblad, On the generators of quantum dynamical semigroups,” *Commun. Math. Phys.* **48**, 119130 (1976).

[79] Y.-Y. Jau, A. Hankin, T. Keating, I. Deutsch, G. Biedermann, Entangling atomic spins with a Rydberg-dressed spin-flip blockade,” *Nat. Phys.* **12**, 71 (2016).

[80] K. Singer, J. Stanojevic, M. Weidemüller, and R. Côté, “Long-range interactions between alkali Rydberg atom pairs correlated to the nsns, npnp and ndnd asymptotes,” *J. Phys. B: Atom. Mol. Opt. Phys.* **38**, S295 (2005); W. Li, D. Viscor, S. Hofferberth, and I. Lesanovsky, Electromagnetically Induced Transparency in an Entangled Medium,” *Phys. Rev. Lett.* **112**, 243601 (2014); D. Cano and J. Fortágh, Multiatom entanglement in cold Rydberg mixtures,” *Phys. Rev. A* **89**, 043413 (2014).

[81] D. Petrosyan, F. Motzoi, M. Saffman, and K. Mølmer, High-fidelity Rydberg quantum gate via a two-atom dark state,” *Phys. Rev. A* **96** 042306 (2017).

[82] M. A. Nielsen, A simple formula for the average gate fidelity of a quantum dynamical operation,” *Phys. Lett. A* **303**, 249 (2002).

[83] A. G. White, A. Gilchrist, G. J. Pryde, J. L. O’Brien, M. J. Bremner, and N. K. Langford, Measuring two-qubit gates,” *J. Opt. Soc. Am. B* **24**, 172 (2007).

[84] E. Knill, R. Laflamme, and G. Milburn, “A scheme for efficient quantum computation with linear optics,” *Nature (London)* **409**, 46 (2001); D.-X. Li, X.-Q. Shao, J.-H. Wu, X. X. Yi, and T.-Y. Zheng, “Engineering steady Knill-Laflamme-Milburn state of Rydberg atoms by dissipation,” *Opt. Express* **26**, 2292 (2018).